EFFICIENCY POTENTIAL SIMULATION FOR AN INDUSTRIALLY FEASIBLE LFC-PERC CONCEPT WITH SENSITIVITY ANALYSIS ON CRUCIAL CELL PARAMETERS

Nico Wöhrle, Johannes Greulich, Martin Graf, Martin Hermle, Stefan Rein
Fraunhofer Institute for Solar Energy Systems
Heidenhofstr. 2, D-79110 Freiburg, Germany
Telephone: +49 761 4588 5075. Fax: +49 761 4588 7621. nico.woehrle@ise.fraunhofer.de

ABSTRACT: PERC solar cells with a rear contact by laser firing (LFC) have shown to be a valid processing concept with a slender process routine and a low metal fraction on the rear side. Nevertheless, if not designed carefully, this solar cell design has a tendency towards pronounced losses at the rear contact area when it comes to comparison with other high efficiency PERC concepts. By applying latest parameterizations for the rear metal contact, we show a detailed free energy loss analysis on numerical simulations. We show that the rear side laser process inducing the high contact recombination is the crucial cell process for improving the LFC-PERC concept. Varying all crucial design parameters, we optimize the rear side design and show sensitivity and strengths of this cell concept including R&D recommendations to reach potential cell efficiencies up to 22.5 %.

Keywords: PERC, Laser Fired Contacts, Simulation, Loss Analysis, Sentaurus Device

1 INTRODUCTION

The laser fired contact (LFC-)PERC cell concept has a key feature when it comes to mass production: It is cheaper to produce compared to other high efficiency PERC routines, especially in comparison with PERC concepts with laser processed local contact openings (LCO)[1]. Nevertheless it hasn't reached a breakthrough in mass production so far. Besides the general challenge to transfer new cell concepts to mass production, the LFC concept in particular shows certain sensitivities to processing parameters such as base resistivity, bulk carrier lifetime and rear contact pitch. In this work we analyze this condition and show valid approaches to reach stable processing windows.

2 THEORY

The rear contact in LFC solar cells is established by firing a metal paste through the rear passivation layer into the silicon bulk using a laser [1], forming a contact and a local Al-BSF beneath it at the same time. In contrast to the LCO concept, where the passivation layer is only opened by a laser beam, the LFC process needs higher laser energy to fire through the metal paste. This has two possible effects: First, it can easily damage the silicon area around the contact. Second, the contact is not flat on top of the silicon, but reaches some micrometers into the silicon in a U-shape, which increases the size of the contact area. The interesting part is now, how this area and the contact itself influence the solar cell performance.

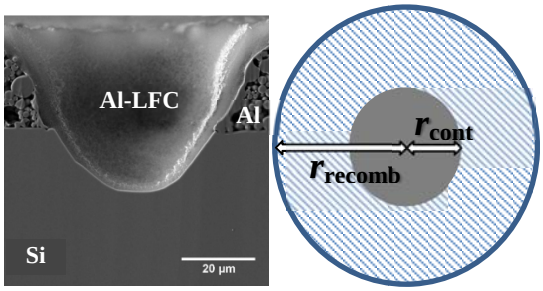

Figure 1: Electron Microscope image of an LFC (left) and top view of contact model with contact radius (r_{cont}) and recombinative radius (r_{recomb}).

A parameterization of the LFCs recombination behavior in terms of the effective surface recombination parameter $S_{met}(N_A)$ was firstly published by in 2008 by Wolf et al. [2]. It models the mentioned increased contact recombination with a circular shaped recombinative area with radius $r_{recomb} = 70$ µm around the circular shaped contact area with radius $r_{cont} = 45$ µm (see Figure 1). The fit curve to measured data for the doping dependence of S_{met} values was found to be of the form

$$S_{met} = S_0 + S_1 \exp\{\beta_{met} N_A\} \quad (1)$$

with the fit parameters S_0, S_1 and β_{met}; and the acceptor density N_A. For PVD aluminum these values were computed to be $S_0 = -10602$ cm/s, $S_1 = 11495$ cm/s, $\beta_{met} = 3 \cdot 10^{-17}$ cm^3 in Ref. [2].
As these values depend on the process conditions, they were recently re-evaluated by Schwab [3] for screen printing the aluminum prior to laser firing. The recombination activity of these contacts was described with the parameters $S_0 = -4404$ cm/s, $S_1 = 4451$ cm/s, $\beta_{met} = 4.75 \cdot 10^{-17}$ cm^3 for $r_{recomb} = 50$ µm and $r_{cont} = 25$ µm. Figure 2 visualizes this correlation.

In the course of the simulation experiment, we will additionally assume a positive development of the laser

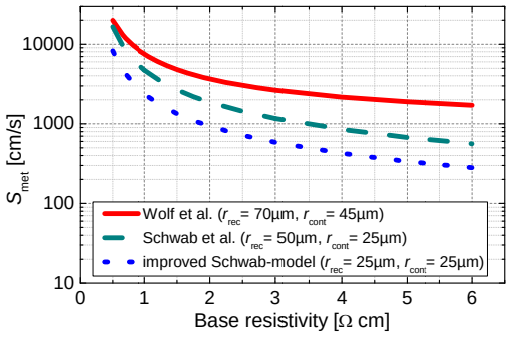

Figure 2: Parameterizations of the surface recombination velocity $S_{met}(N_A)$ at the LFC metal-silicon interface by Wolf (PVD-Al) and Schwab (Screen-printed Al), and the improved LFC parameterization.

[1] as a result of internal calculations.

Table I: Parameter variations in the LFC simulation

Parameter	Unit	Variation
Base resistivity ρ	Ω cm	0.5 / 1 / 1.5 / 2.5 / 6
Rear Pitch	µm	200 / 300 / 400 / 500 / 600
Bulk carrier lifetime τ_{bulk}	ms	0.2 / 0.5 / 1 / 2

firing process. We have reason to believe this is possible, as it is a matter of laser technology currently being addressed for LCO laser processes, called "pulse shaping" [4], with the option to transfer it to the LFC process. By this we see a possible avoidance of the damage area around the actual contact and an avoidance of the U-shape of the contacted area size by firing shallower contacts. So in the improved LFC setup we assume $r_{recomb} = r_{cont.}$ We also assume an improvement of the S_{met}-value by factor of two leading to the formula

$$S_{\mathrm{met}} = \frac{1}{2}\left(S_0 + S_1 exp\{\beta_{met} N_A\}\right) \quad (2)$$

with the parameter values of Schwab [3].

For analyzing energy losses we use the method of "Free Energy Loss Analysis" (FELA). With its help loss mechanisms in solar cell devices are calculated all by same units (mW/cm²), so different loss channels stay directly comparable. FELA was first introduced 2008 by Brendel et al. [5] and extended by Greulich et al. [6] in 2013. As the electrical power, the analyzed Free Energy fluxes are free of entropy. FELA is a locally resolved method and is therefore suitable to quantify loss mechanisms for each region of interest separately, e.g. the emitter, the surface, or the base.
The bars in the FELA plots of the present work show power loss at maximum power point (MPP) of the particular solar cell. It is important not to directly conclude to cell power output from this, as the MPP varies from cell to cell. Therefore the generated free energy P_{gen} (= potential electrical power of the cell) and the actual electric power output P_{IV} are attached in each FELA plot. The difference between P_{gen} and P_{IV} yields the sum of the loss bars.

3 SIMULATION SETUP

A three dimensional LFC-PERC symmetry element was built for numerical simulations using Sentaurus Device [7] and state-of-the-art models [8]. This *p*-type Si cell has a thickness of 180 µm. It features a high-performance boron emitter with a sheet resistance of 85 Ohm/sq and a dark saturation current density of j_{0e} = 50 fA/cm².

The laser fired contacts at the rear are parameterized as described in Section 2 with a recombination radius r_{recomb} twice the size of the point contact radius r_{cont} = 25 µm.

In the simulation experiment, we vary the parameters contact pitch, base resistivity, and bulk carrier lifetime, as displayed in Table I. To represent resistive losses in the metallization, we use a lumped external resistance of 0.5 Ωcm² for all the simulations. The metallization is not part of the improvement considerations in this work. We set our focus on bulk and rear contacts.

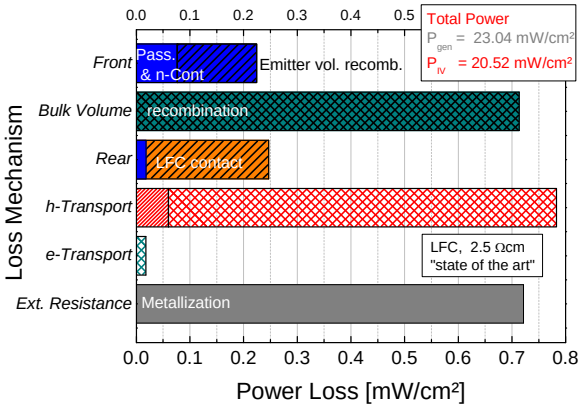

Figure 3: FELA of state of art LFC cell at 2.5 Ωcm and 0.2 ms bulk lifetime. Region labels: emitter (striped), base (diamond-patterned).

Optics-wise the carrier generation was calculated for random pyramids and a 75 nm thick anti-reflection-coating (SiN_x). For the rear side we used a planarized surface with a remaining roughness, calculated with the tilted mirrors model [10, 11] assuming a passivation stack of 10 nm AlO_x and 75 nm SiN_y covered with aluminum. This yields a photo generation current of 40.07 mA/cm². To keep the electrical effects of the experiment observable, the same optical generation is used for all simulations.

The following list intends to provide a comprehensible overview of the simulation steps we take:

1) Simulation of a state-of-the-art cell, i.e. comparable to recently published results, e.g. [12, 13]. That means S_{met} parameters from eq. (**1**) and, according to Schwab [3], $r_{recomb} = 2\ r_{cont}$. Nevertheless this cell has still higher efficiency than the published results on large area cells, as we use the high performance emitter mentioned above for comparability reasons (see section 4.1).
2) Simulation of the performance with improved S_{met} parameters (eq. (**2**)) and $r_{recomb} = r_{cont}$ (see section 4.2)

In every step, we vary the parameters base resistivity, rear contact pitch and bulk carrier lifetime according to the values listed in Table I and perform a FELA.

4 RESULTS

4.1 State-of-the-art LFC setup

This cell is simulated with a bulk lifetime of 200 µs. The results can be seen in Figure 4.

Ignoring extreme values of pitches larger than 500 µm combined with ρ = 6 Ωcm, they show efficiencies between 19.5 and 21.5 % (Figure 4). The efficiency loss from large towards small contact pitches at low base resistivity, originating from j_{SC} losses, are with $2\%_{abs}$ tremendous. They get smaller with higher resistivity, but in turn therefore the FF drops, leading to even bigger efficiency losses. So, we see two opposing effects influencing the overall efficiency. In the graphs of Figure 4, efficiency, j_{SC}, V_{OC} and FF are plotted to give orientation, how the IV-parameters change in this setup for different contact pitches and base resistivities.

Now we look at the loss analysis in Figure 3, which was taken at 500 µm pitch and 2.5 Ωcm base resistivity. This point is chosen as we see a lot of cells in R&D being

produced with material around 2.5 Ωcm as it is largely available and people tend to seek a compromise between a low resistivity (low spreading resistance) and low boron doping (less BO-defects), which increases carrier lifetime.

The FELA graphs are designed as follows: The x-axis shows power loss in mW/cm². This unit allows us to translate these numbers directly to efficiency gain. On the y-axis, the top column shows front side recombination losses, divided into pure surface losses (passivation & n-contact) and losses in the emitter volume (striped). The second (green) column denotes the recombination loss in the base volume. The third column shows the rear side losses with passivation (blue) and contact recombination losses (spreading resistance excluded). The fourth and fifth column show hole- and electron transport losses in the emitter (striped) and in the base (diamond-patterned). The last column shows the extenmal metallization losses of fingers and busbars.

The FELA of Figure 3 shows that in this case the loss mechanism accounting most is the hole (majority carrier) transport loss in the base, also known as "spreading resistance" (R_{spread}). This effect originates from the need of the majority carriers for a lateral movement in the base to reach the point-shaped rear contacts since a highly conducting full-area back-surface-field is absent. Together, spreading resistance and bulk recombination effects cause a power loss of 1.4 mW/cm² or 1.4%$_{abs}$ in efficiency allowing for a solar cell efficiency of 20.5 %, j_{SC} = 39.8 mA/cm², V_{OC} = 663 mV, and FF = 78 %.

Now, we reduce the base resistivity to 0.5 Ωcm, which cuts down the spreading resistance losses to 0.15 mW/cm² and the bulk recombination to 0.33 mW/cm² as Figure 5 shows. So, we gain efficiency only from switching the base resistivity if the lifetime can be kept at 200 µs. Not visible in this plot is that V_{OC} raises as well, giving the cell a total gain of 1 %$_{abs}$ in efficiency. The solar cell efficiency is now 21.5 %

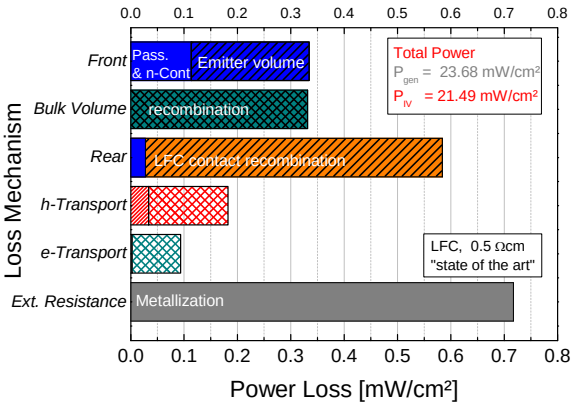

Figure 5: FELA of state of art LFC cell at 0.5 Ωcm and 0.2 ms bulk lifetime.
Region labels: emitter (striped), base (diamond-patterned)

(j_{SC} = 39.4 mA/cm², V_{OC} = 673 mV, FF = 81 %). While the bulk and transport losses are reduced, the rear contact loss losses are more than doubled to 0.58 mW/cm². We will focus on this in the discussion.

4.2 Improved LFC setup

As a next step we want to see, which effect the removal of the recombinative the area around the rear contact ($r_{recomb} = r_{cont}$) and improved S_{met} parameterization (see eq. (**2**)) have, while leaving the bulk lifetime at 200 µs.

We see in Figure 6, that this has a huge effect on the rear contact losses, reducing them to 0.21 mW/cm². In turn, the front and the bulk volume recombination losses increase by 0.17 mW/cm² each to 0.5 mW/cm² each. The cell's efficiency still raises to 22.04 %, because the generated free energy also sees a gain. In terms of IV-parameters, the reason is mainly the FF gain of three percentage points.

As a final step, to address the increased bulk recombination, we have a look at the effect of increased carrier lifetime, setting τ_{SRH} to 2 ms. Here the bulk recombination is reduced by 0.35 mW/cm² leading to a 10 mV gain in V_{OC}, 0.1 mA/cm² in j_{SC} and 0.4 %$_{abs}$ in FF; resulting in efficiency gains of 0.5 %$_{abs}$. This leaves us with the final result of a 22.5% efficient LFC cell, originating from the IV-parameters V_{OC} = 693 mV; j_{SC} = 39.8 mA/cm² and FF = 81.5 %. Figure 8 pictures the associated IV-parameters.

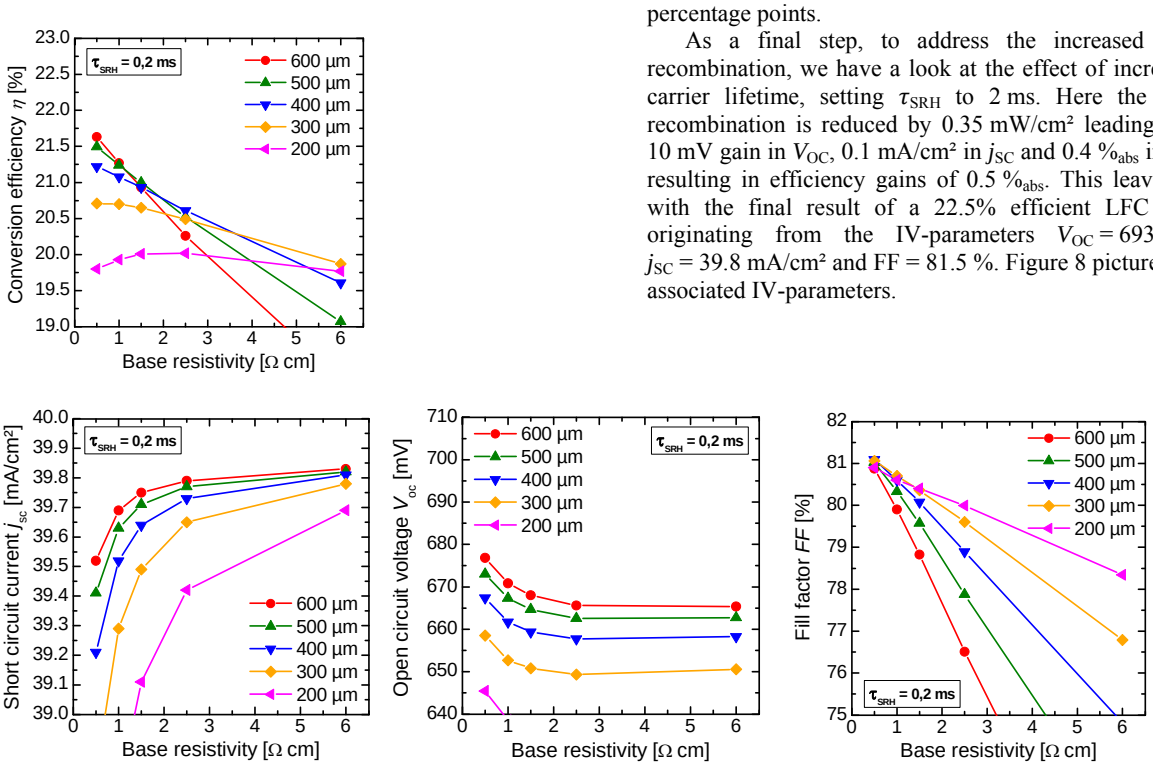

Figure 4: State of art LFC cell with damaged area around rear contacts. Variation of base resistivity and contact pitch.

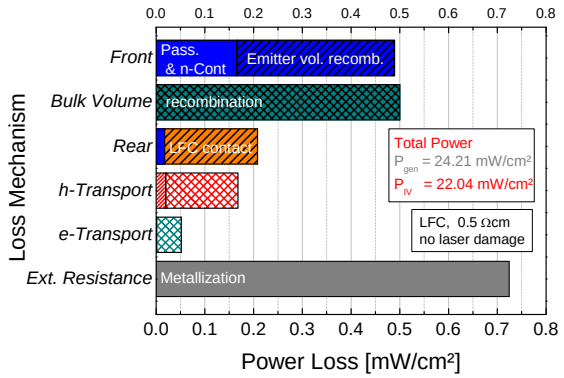

Figure 6: FELA of improved LFC cell ($r_{recomb} = r_{cont}$) at 0.5 Ωcm and 0.2 ms bulk lifetime. Region labels: emitter (striped), base (diamond-patterned)

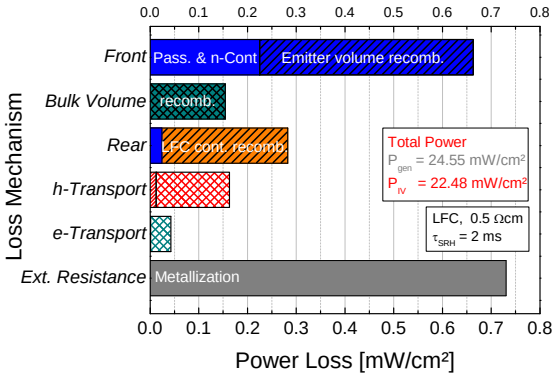

Figure 7: FELA of improved LFC cell ($r_{recomb} = r_{cont}$) at 0.5 Ωcm and 2 ms bulk lifetime. Region labels: emitter (striped), base (diamond-patterned)

5 DISCUSSION

As pointed in section 4.1 for $\rho = 2.5$ Ωcm, the major power loss comes from the bulk volume and spreading resistance due to current crowding. This loss cannot be compensated by reducing the pitch, as this leads to higher contact coverage of the rear side. The so caused increase in contact recombination forces a V_{OC} drop of roundabout -30 mV going from 500 µm to a 200 µm pitch.

In terms of the IV-curve the power loss of 1.4 mW/cm² or 1.4%$_{abs}$ in efficiency originating from the spreading resistance and bulk recombination bar are exclusively FF losses. Figure 4 acknowledges this, if you compare the FF-plot at 2.5 and 0.5 Ωcm.

At this point (see Figure 5), the bulk losses with 0.33 mW/cm² and the hole transport losses (0.18 mW/cm²) are minor. This is the first biggest issue to be addressed when optimizing LFC cells (or in general local BSF cells): Provide for excellent lateral conductivity in the base by seeking high base doping! This is especially neccessary when dealing with low and moderate bulk lifetimes ($\tau_{SRH} < 1$ ms).

We notice the other remarkable effect if we turn our attention towards the recombination losses at the rear contact interface in Figure 5. Coming from 2.5 to 0.5 Ωcm, we observe more than a doubling of the recombination losses from the rear contact. This is quite important for one reason: Besides the increasing S_{met} values for higher base doping, in the former setup the losses in the base (bulk recombination & R_{spread}) were so massive, that there were not enough carriers left to exploit the full loss potential of the contact and the laser damaged area around it. Now that the bottleneck of base recombination losses is minimized, we notice, that, except for external metallization losses, the rear contact area of the rear contact/silicon interface is by far the largest power stealer; which is the second important cognition on the way to an excellent LFC solar cell. To generalize this: The extent to which loss mechanisms strike depends not only on the quality of the single solar cell component, but heavily on the balance of different parts of the cell.

That is the reason why we now focus on the rear contacts, now being the biggest power consumer with 0.58 mW/cm² power loss. Reducing or avoiding the damage induced by the laser process forming the contact is now the crucial point to further improve the LFC cell's performance. The optimization of the rear contact by minimizing the laser damaged area shifts the majority of

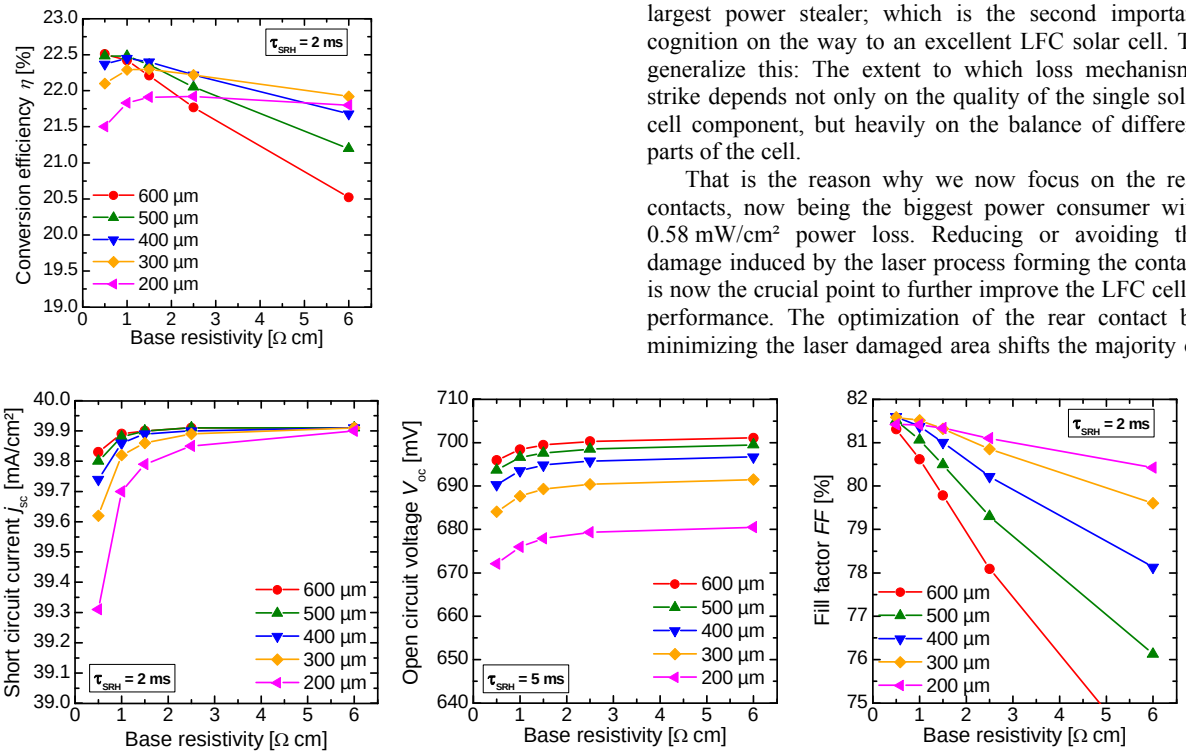

Figure 8: Improved LFC cell at 0.5 Ωcm without damaged area around rear contacts. Variation of base resistivity and contact pitch

losses back to the bulk – and even more to the front surface and the emitter volume, which can be observed in Figure 6.

Improvement of the material quality again is a quite obvious step in optimizing solar cells. The new part here is, that FELA can show and quantify the detailed impact of it, comparing Figure 6 and Figure 7:

Bulk volume recombination is reduced from 0.50 to 0.15 mW/cm². This again frees bound carrier resources that now recombine partially at the front (emitter volume & surface) instead, raising its loss from 0.50 to 0.66 mW/cm². We also see that a small amount of the losses shifted back to the rear side. As the free energy generation P_{gen} also increases from 24.21 to 24.55 mW/cm², which means we subtract the losses from a higher generation level, we get an overall power generation of 22.48 mW/cm² or an efficiency of about 22.5 %.

The parameter variations of Figure 8 show the sensitivity of the optimized LFC cell concept. We see that compared to the initial situation (Figure 4) the sensitivity towards changes of base resistivity are reduced heavily. Where the best pitches of 500 and 600 µm formerly lost more than 0.5 % efficiency between 0.5 and 1.5 Ωcm, they now barely lose 0.2 %. For 400 and 500 µm pitch, the LFC concept is now stable above 22.0 % efficiency up to a resistivity of 3 Ωcm.

This leaves us with two more findings:

1) The next step would be optimizing the front of the solar cell (emitter and its passivation and metallisation). Although this is a quite important topic, it is not LFC specific, but of interest for all front junction cell concepts. So here, we would leave the path of bringing the LFC concept up front.
2) Solar cell research means iterative development, facing and minimizing the tightest bottleneck – one after the other. The weaknesses of all the single pieces of those complex high efficiency cells superpose each other to an extent that solving them layer by layer is a promising strategy. Solar cell simulation offers the opportunity to gain access to the physical processes taking place and catalyze the optimization routines sustainably.

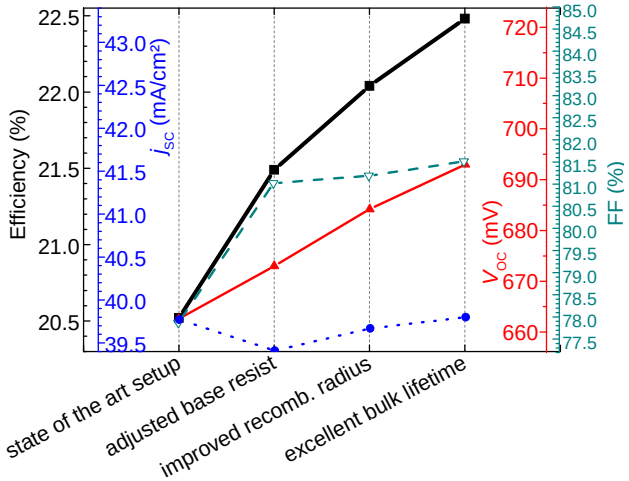

Figure 9: Improvement curve of LFC cell simulation

Figure 9 finally shows the overall changes in IV-parameters, which result from the three optimization steps. For highest enjoyment, the axes are scaled to relative equality. That means a change of 1%$_{rel}$ in j_{SC}, V_{OC}, or FF, appears graphically as large as a 1%$_{rel}$ change in efficiency.

6 CONCLUSION

As a result of the simulation of an LFC-PERC solar cell concept we can conclude the following points.

Improving a high efficiency solar cell means removing power loss bottlenecks step by step. This seems obvious but is nevertheless very important as bottlenecks disguise other potential loss mechanisms.

The first important step is going for low base resistivities of 0.5 Ωcm while keeping the minority carrier lifetimes moderately high as shown here for 0.2 ms, otherwise the spreading resistance and bulk volume recombination will limit the cell. If you try to escape this by narrowing the rear side contact pitch (here 200 µm), losses due to recombination at the LFCs limit the cell to 20 % efficiency at moderate lifetimes of 0.2 ms. High lifetimes of around 2 ms provide higher flexibility concerning pitch and base resistivity.

In the second step, take good care of the laser process of the LFCs. After choosing the right base resistivity in the first step, the rear contact areas are the largest source of power loss in the LFC cell. Reduce the laser induced damage to the area of electrical contact between silicon and aluminum as far as possible and achieve a flat contact shape; in return one will receive a V_{OC} gain in the size of 10 to 25 mV (pitch depending). This allows for cell efficiencies well above 21.5 %, even for bulk lifetimes of 0.2 ms. Choose the best material you can get, to let the cell reach up to 22.5 % conversion efficiency (here at 2 ms bulk lifetime).

At this point, our chosen 50 fA/cm² emitter has become the bottleneck of the LFC cell. This triggers the next logical step in the concept's evolution, but emitter development is not directly LFC related anymore.

To this detail, the investigation of losses in a solar cell is not possible without simulation playing a major role. Multi-dimensional simulation with highly customizable output parameters opens the door to distinguishing between the different loss mechanisms and splitting them into different loss channels and regions.

6 ACKNOLEDGEMENTS

N. Wöhrle gratefully acknowledges the scholarship of the German Federal Environmental Foundation ("Deutsche Bundesstiftung Umwelt").

The authors would like to thank Gabriel Micard (University of Konstanz) for the helpful discussions about calculation of transport losses.

7 REFERENCES

[1] E. Schneiderlöchner, R. Preu, and R. Lüdemann, et al, "Laser-fired contacts (LFC)," in *17th EUPVSEC Munich*, 2001, pp. 1303–1306.

[2] A. Wolf, D. Biro, and J. Nekarda, et al, "Comprehensive analytical model for locally contacted rear surface passivated solar cells," *Journal of Applied Physics*, vol. 108, no. 12, p. 124510, 2010.

[3] C. Schwab, "Herstellung und Charakterisierung industrieller oberflächenpassivierter p-typ Solarzellen," Dissertation, Fraunhofer Institut für Solare Energiesysteme ISE, Albert-Ludwigs-University, Freiburg, 2013.

[4] A. Brand, F. Meyer, and J. Bartsch, et al, "Tailored Low Damage Laser Contact Openings for Large Area High Efficiency Solar Cells," in *29th EUPVSEC Amsterdam*, 2014, to be published.

[5] R. Brendel, S. Dreissigacker, and N.-P. Harder, et al, "Theory of analyzing free energy losses in solar cells," *Appl. Phys. Lett,* vol. 93, no. 17, p. 173503, 2008.

[6] J. Greulich, H. Höffler, and U. Würfel, et al, "Numerical power balance and free energy loss analysis for solar cells including optical, thermodynamic, and electrical aspects," *J. Appl. Phys,* vol. 114, no. 20, p. 204504, 2013.

[7] Synopsys, "Sentaurus Device User Guide," in *Sentaurus Manuals: Inspect, Structure Editor, Sdevice, Tecplot, Svisual, Inspect*, Synopsys, Ed. 2012nd ed, 2012.

[8] P. P. Altermatt, "Models for numerical device simulations of crystalline silicon solar cells—a review," *J Comput Electron*, vol. 10, no. 3, pp. 314–330, 2011.

[9] F. Book, A. Dastgheib-Shirazi, and G. Hahn, et al, "Detailed Analysis of High Sheet Resistance Emitters for Selectively Doped Silicon Solar Cells," in *24th EUPVSEC Hamburg*, 2009.

[10] N. Wöhrle, J. Greulich, and C. Schwab, et al, "A Predictive Optical Simulation Model for the Rear-Surface Roughness of Passivated Silicon Solar Cells," *IEEE J. Photovoltaics*, vol. 3, no. 1, pp. 175–182, 2013.

[11] J. Greulich, N. Wöhrle, and M. Glatthaar, et al, "Optical Modeling of the Rear Surface Roughness of Passivated Silicon Solar Cells," in *SiliconPV 2012*: Elsevier, 2012, pp. 234–239.

[12] A. Wolf, E. A. Wotke, and A. Walczak, et al, "Pilot line processing of 18.6% efficient rear surface passivated large area solar cells," in *35th IEEE Photovoltaic Specialists Conference*, 2010.

[13] C. Schmiga, M. Rauer, and M. Rüdiger, et al, "Aluminium-doped p+ silicon for rear emitters and back surface fields: results and potentials of industrial n- and p-type solar cells," in *25th EUPVSEC Valencia*, 2010.